Univerza v Ljubljani
Faculty of mathematics and physics
Department of physics

Jadranska cesta 19
1000 Ljubljana

Ljubljana, 13. 3. 2001

How to increase lift of an airfoil

Author: Luka Vidic
Adviser: prof. dr. Rudolf Podgornik

1 Abstract

It is in human nature to explore more effective and economical techniques, which make things work better. In this seminar we will explore the possibilities of increasing the lift, produced by an airfoil, by different methods. First we will determine the variables, on which the lift coefficient depends, and we will later use this knowledge to explore the high lift devices. The main goal of this seminar is also to show, that a lot of solutions to our problems already exist in the nature as a consequence of evolution.

Contents

2 Introduction

Since wings are main topic of this seminar, it is essential to explore the terminology of wing, which will be used in the following sections [1, p.115].

The wing profile on the figure 1 has a *leading* and a *trailing end* at points B and A

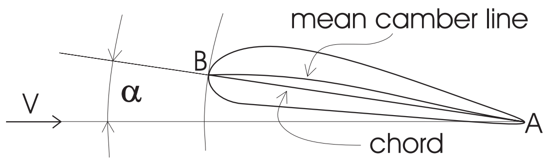

Figure 1: Terminology of the wing profile

respectively. Point B is given as a one point cross-section of the profile and the arc with its centre in the point A. The straight line bonding A and B is called the *chord.* The angle defined by the direction of velocity of an undisturbed fluid and the chord is the *angle of attack.* If we draw lines perpendicular to the chord from upper to lower border of the profile and mark them with midpoints, then the bent line binding them inside the profile is *mean chamber line.* This line denotes the symmetry of a wing according to the chord. *Camber* is the maximum value of distance between the chord and the mean chamber line. *Thickness* is the length of the largest line, used to gain the chord.
In this seminar, we will discuss velocities, lower than the speed of sound.

3 Lift coefficient

There are three basic coefficients in the theory of airfoils: lift, drag and moment. In this seminar, we will explore the lift coefficient C_L. Using C_L, the amount of lift produced by an airfoil can be found as [1, p.114]:

$$L = \frac{\varrho}{2} V^2 S C_L \quad ,$$

where V denotes the velocity of an undisturbed stream, ϱ the density of the fluid, and S the airfoil area ($S = bc$), where b denotes the wingspan, and c the chord length.

Through exploring the characteristic properties of wing profiles, it has been shown [1, p.139], that the values of all three coefficients depend on the shape of the profile, the angle of attack α, the aspect ratio of the airfoil $AR = b/c$, and the Reynolds number Re.

3.1 Lift coefficient of a thin airfoil

Although coefficients are mostly gained from experimental results, it is possible to get their theoretical approximation. In order to obtain analytical result for lift coefficient, we will discuss thin airfoils [1, p.201] under a small angle of attack and of infinite aspect ration (two-dimensional approximation). That means that both camber and thickness will have small values in relation with the chord. Even more, we will use infinitesimal thickness, so that the whole profile will deform into a single curve – the mean camber line (figure 2).

According to W. M. Kutta, an approximate solution for a thin airfoil with two sharp

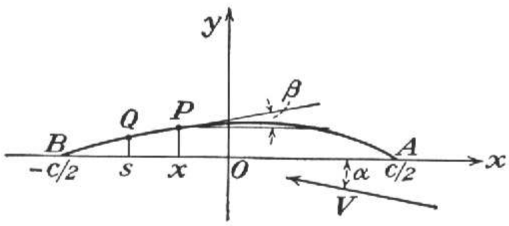

Figure 2: Thin airfoil [1]

edges, under a small angle of attack, can be found by considering the irrotational flow with finite velocity at the trailing end but infinite velocity at the leading end [1, p.200]. Any kind of flow around an 2D airfoil can be represented as a superposition of an uniform motion and a number of circulating motions with different centre points [1, p.189]. Our circulating motions will actually be represented by a uniform vortex sheet (appendix 10), [1, p.191] Let us therefore explore the circulation Γ of the flow[1] around the thin airfoil. If Γ' denotes the vortex density (appendix A), we can write:

$$\Gamma = \oint_K v(s)\mathrm{d}s \qquad \mathrm{d}\Gamma = \Gamma'\mathrm{d}s \tag{1}$$

Kutta's condition stipulating a finite velocity at the trailing end implies that the vortex density is zero there. In addition, the distribution of Γ' over the sheet is the subject to the condition that there is no resulting flow across the mean camber line C.

Let V denote the magnitude of the velocity of the undisturbed stream and α the angle of attack. If a slope of the mean chamber line is at a given point $\beta = \mathrm{d}y/\mathrm{d}x$, then the velocity component, normal to C, has the magnitude $V\sin(\alpha+\beta) \approx V(\alpha+\beta)$. Γ' must be determined so that for any point on C, this normal velocity component will be canceled. In low order approximation, we can deduce, that the induced velocity equals

[1] K denotes a closed curve, s is the element of length

the quotient $\Gamma'(s)\mathrm{d}s$ divided by 2π times the distance ($\overline{PQ} = x - s$).
For a given function $\beta(x)$, defined in the interval $-c/2 \leqq x \leqq c/2$, we must therefore determine Γ' so that

$$\begin{aligned} \Gamma'\left(-\frac{c}{2}\right) &= 0 \\ \frac{1}{2\pi}\int_{-c/2}^{c/2} \frac{\Gamma'(s)\ \mathrm{d}s}{x - s} &= -V[\alpha + \beta(x)] \end{aligned} \tag{2}$$

If this problem is solved, the lift coefficient is found according to Kutta-Joukowsky theorem[2] [4, p.56]:

$$\begin{aligned} C_L &= \frac{2}{\varrho V^2 c}\, L \;=\; \frac{2}{\varrho V^2 c}\, \varrho V \Gamma \\ &= \frac{2}{Vc}\int_{-c/2}^{c/2} \Gamma'(s)\ \mathrm{d}s \end{aligned} \tag{3}$$

The problem of determining coefficient of lift is reduced to finding the vortex density Γ' which satisfies the conditions (2).
In order to solve this problem, it is helpful to replace variables x and s by new variables defined by

$$\frac{2x}{c} = -\cos\varphi\ , \qquad \frac{2s}{c} = -\cos\vartheta$$

Equations (2, 3) now take form:

$$\Gamma'_\vartheta = 0\ ;\quad \vartheta = 0 \tag{4}$$

$$\frac{1}{2\pi}\int_0^\pi \frac{\Gamma'_\vartheta\ \sin\vartheta\ \mathrm{d}\vartheta}{\cos\vartheta - \cos\varphi} = -V(\alpha + \beta_\varphi) \tag{5}$$

$$C_L = \frac{1}{V}\int_0^\pi \Gamma'_\vartheta\ \sin\vartheta\ \mathrm{d}\vartheta \tag{6}$$

The general case can be treated by assuming that the vortex density Γ' can be represented as a sum of the form

$$\Gamma_\vartheta = 2V\left(\Gamma'_0 \frac{1-\cos\vartheta}{\sin\vartheta} + \Gamma'_1 \sin\vartheta + \Gamma'_2 \sin 2\vartheta + \cdots + \Gamma'_n \sin n\vartheta\right) \tag{7}$$

where the constants Γ'_i should be determined by the shape of the mean camber line. Expression (7) obviously satisfies the first condition (4). Now we will show the relation of Γ'_i with the profile. In order to accomplish this, we will use the following integral formulas:

$$\int_0^\pi \frac{\mathrm{d}\vartheta}{\cos\vartheta - \cos\varphi} = 0$$

[2]The lift force of a wing equals the product of fluid density, magnitude of velocity in an undisturbed stream and the circulation around an airfoil. We also replaced the wing area S with the chord c, since we are trying to determine the 2D solution (wingspan b is not relevant)

$$\int_0^{\pi} \frac{\cos\vartheta \;\mathrm{d}\vartheta}{\cos\vartheta \;-\; \cos\varphi} \;=\; \pi$$

$$\frac{1}{\pi}\int_0^{\pi} \frac{\sin n\vartheta \;\sin\vartheta}{\cos\vartheta \;-\; \cos\varphi}\,\mathrm{d}\vartheta \;=\; -\cos n\varphi$$

Upon substituting (7) in the equation (5), it will take the form

$$\sum_{i=0}^{n} \Gamma_i' \cos(i\varphi) \quad = \quad \alpha \;+\; \beta_\varphi$$

Without restricting the generality of the discussion, the function β_φ can be represented by a sum of the form

$$\beta_\varphi = \sum_{i=0}^{n} \beta_i \cos(i\varphi)$$

where the constants β_i depend on the shape of the mean camber line. Comparing the last two equations, we see that the following conditions must be fulfilled:

$$\Gamma_0' \;=\; \alpha + \beta_0 \quad ; \qquad \Gamma_i' = \beta_i \;, \quad i = 1, 2, \ldots, n \tag{8}$$

Let us now try to determine the analytical result for C_L. In order to do that, we will use this integral equation:

$$\begin{aligned} \int_0^{\pi} \sin p\vartheta \;\sin q\vartheta \;\mathrm{d}\vartheta \;&=\; 0 \;;\quad p \neq q \\ &=\; 1 \;;\quad p = q \end{aligned}$$

Using all given results, we can obtain the following value of the lift coefficient:

$$\begin{aligned} C_L \;&=\; 2\pi\;(\alpha + \beta_0) \;+\; \int_0^{\pi} \left(\sum_{i=1}^{n} \beta_i \sin(i\vartheta) \right) \sin\vartheta \;\mathrm{d}\vartheta \\ &=\; 2\pi \left(\alpha \;+\; \beta_0 \;+\; \frac{\beta_1}{2} \right) \end{aligned} \tag{9}$$

Let us explore this result a little further. We can see, that C_L is a function of the shape of the profile (β) and the angle of attack (α). The Reynolds number[3] does not stand as a direct parameter in the given result (9). We will discuss its role later.

The result shows that the slope of the C_L vs. α-curve is constant, independently of the shape of the profile, while the zero lift angle $\alpha_0 = -\beta_0 - \beta_1/2$ depends on the shape. It is also very important to notice, that a symmetrical wing ($\beta_i = 0$ will also produce lift when shifted for a certain angle of attack.

[3]Reynolds number $Re = \varrho V l/\eta$ represents only the change of velocity v in our case. Due to subsonic velocities the density (ϱ) remains constant and so does the viscosity (η). The shape constant of length l also does not change, therefore the only thing that will change the value of Re is velocity.

3.2 Experimental results

3.2.1 Angle of attack

As we discovered before, each profile produces zero lift at certain angle of attack α_0. If the angle of attack is measured from the chord, the angle α_0 will be negative for the usual profiles. The figure (3) shows empirical results, obtained in the wind tunnel with a wing of constant profile. The first observation could lead us to think that for moderate

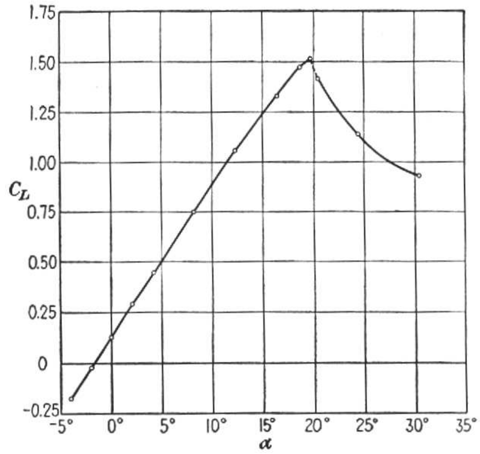

Figure 3: C_L vs. α diagram of the profile NACA 2409 [1]

values of angle of attack, the lift coefficient is proportional to $\alpha' = \alpha - \alpha_0$. However, more precise experiments show, that the C_L vs α-curve is slightly bent, so that formula

$$C_L = k \sin \alpha'$$

may be considered a slight improvement.

The upper point of the curve is called the *stalling point*[4]. From that point further, the lift coefficient decreases with increasing angle of attack. Why does this happen? The answer lies in the boundary layer. The fluid has zero velocity on the surface of the wing. Due to viscosity of the fluid, it slows the fluid in the layer above it. A boundary layer is a layer of thickness, in which the velocity will gain 96% of the velocity of undisturbed flow. The air in the boundary layer will at slow speed (or large angle of attack) gradually lose kinetic energy due to friction faster than at small angle of attack. Therefore, they will not be able to sustain the laminar flow, which will result in flow separation. As observed on the diagram (3), the lift coefficient decreases rapidly.

[4] At this point the streamlines start to separate from the wing. This will result in rapid decrease of lift coefficient and therefore in produced lift. The plane can lose the ability to fly

3.2.2 Influence of aspect ratio

The experimental values of the slope of the C_L vs. α-diagram for the usual wing profiles are fairly well represented by

$$k = \frac{0.1}{1\ +\ 2/AR}$$

if α is expressed in degrees. Figure (4) shows the experimental curves obtained with

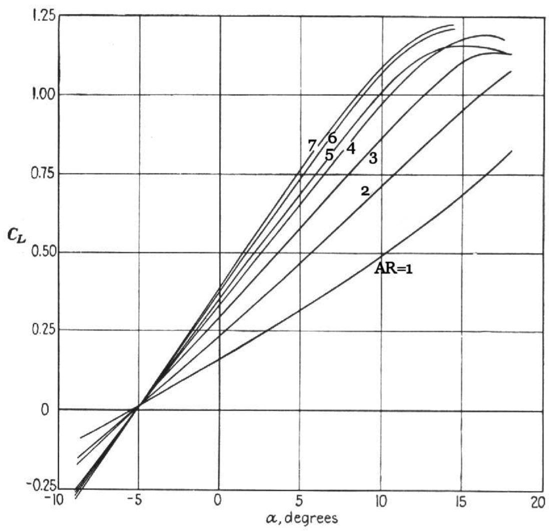

Figure 4: Lift curves of airfoils for various aspect ratios [1]

airfoils of the same profile but of different AR. The linear portions of these curves clearly have different slopes. The value for maximum lift coefficient increases with increasing AR from 1 to about 3, and then remains almost constant. The typical values of AR are small (around 3) for supersonic aircraft, and from 6 to 12 for commercial aircraft.

3.2.3 Influence of profile

The experiments on the so called four digit NACA family of airfoils show that the slope k of the straight portion of curve C_L vs. α decreases slightly with increasing thickness and is almost independent of the camber [1, p.162]. Those changes are however very small. Experimental results show a variation of k from $k = 0.103$ for the relative thickness $t/c = 0.06$ to $k = 0.097$ for $t/c = 0.21$ These are values for an airfoil with the camber designation 24 (camber/c=0.02; maximum at 40% length aft of the leading end). For an airfoil of camber designation 64 the corresponding k-values are 0.104 and 0.096.
The two dimensional airfoil theory does not predict a decrease of k with increasing thickness. Therefore it seems, that this discrepancy is probably due to effects of viscosity. The

position of the maximum chamber does however take effect on the size of the no-lift angle of attack.

3.2.4 Influence of Reynolds number

For the airfoils the chord length is usually taken as the reference length in defining the Reynolds number. Although we must admit, that the conditions in the wind tunnel are far too perfect according to reality (turbulence, finite AR), we are able to get satisfying results. Thus we can determine, that the slope k of the straight portion of the lift-angle curve increases slightly with Re. However, the theoretical values cannot be reached, probably due to viscosity. The maximum value of C_L can be increased (figure 5) by increasing Re, but not at high values of Re, where turbulent motion and separation of fluid from the wing would occur.

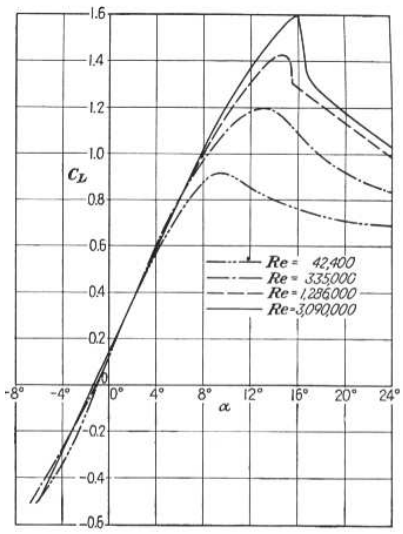

Figure 5: Change of slope and maximum value of C_L at different Re. [1]

4 High lift devices

In order to achieve higher values of lift coefficient at given circumstances, we must make use of our understanding the phenomenon of flight. We will see, that a lot of mechanisms, that man invented , in this case already exist in the nature as a result of evolution.

4.1 Mechanical devices

The early attempts of increasing the lift force, induced by the wing in the velocity field of a fluid, based on the Kutta-Joukowsky theorem

$$L = \varrho V \Gamma.$$

As we can do very little about the density of the fluid, we can obtain higher values of lift by increasing velocity of an aeroplane, or by increasing the circularity Γ.
This can be done by increasing the speed of fluid on the upper side of the wing and reducing it on the lower side. That will increase the propelling (kinetic) energy of the boundary layer and also increase the its stability in terms of flow separation. Figure (6) shows wings with moving surfaces as one of the possibilities of mechanical increased lift force. Although this devices have been tested, they have never been used on real airplanes as means of increasing the lift. Other way of increasing the energy of the boundary layer

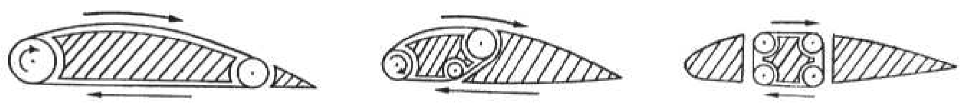

Figure 6: Tokaty's wings [2]

particles is injecting a thin jet of air through a spanwise slit in the upper surface of the wing (figure 7,a). Experimental values of C_{Lmax} up to 3.3 have been observed [1, p.266].

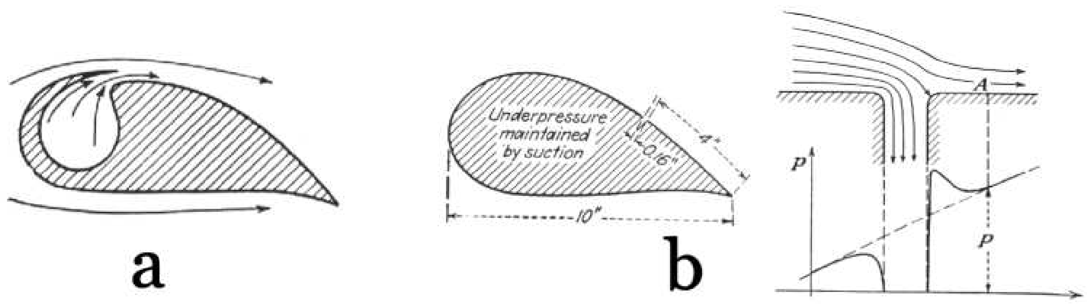

Figure 7: Boundary layer control by pressure slot [1]

The other method bases on removing the low energy air from the boundary layer by a suction through a porous surface or a slit. As the low energy air is sucked into the wing, "new" air, previously undisturbed by friction, will come into boundary layer from above (figure 7,b). As it has previously not encountered boundary friction, it will have more kinetic energy than the former air. In other words, we have created a stable pressure difference between the stagnation point on the leading end and the flow over the trailing end. This method also has not been used in the way described, but has been a good start-up point for further development of high lift devices.

4.2 Flaps and slats

Let us examine the possibility of creating high lift coefficients at small velocities. We already know from the section 3.2.1, that stalling occurs at low velocities. How to prevent this from happening? In the section 4.1 we examined injection of air into a boundary layer. Can that also be achieved just with changing the structure of wing profile? As that would be more economical, we must pursue this task further.
We are learning to fly for a little more then a century. But birds and insects have mastered this ability long ago. Is it not obvious, that we should look for the mechanisms which nature invented over a systematic phenomenon of evolution.
If one observes birds when flying at low velocities (at landing), one may observe, that

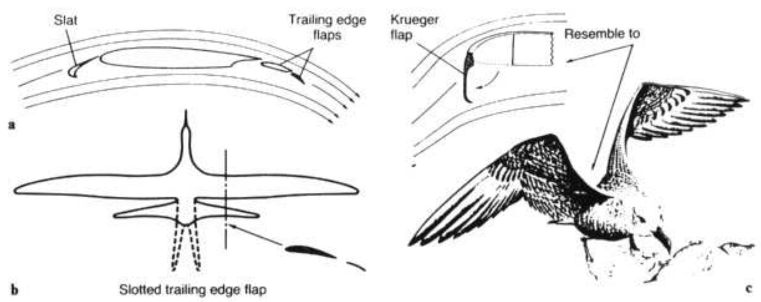

Figure 8: Flaps constructed by nature [3]

their wings become deformed in such manners, that some parts, previously hidden, come to use. One of such parts is called alula (figure 9) or the bastard wing. It is a set of 3 to 5 feathers that form an aileron in front of the main wing. If we look at the gliders (albatros, seagull), we can also observe, that they spread the tail feathers (figure 8,b) which thus form another set of ailerons close to the trailing end of the main wing, similar to what we call flaps. There are two contributions of flaps and slats to increasing the lift coefficient. The first is deformation of wing profile, which becomes more cambered. Simultaneously, the effective angle of attack increases by this deformation, generating more lift. But we know, that at high angles of attack stalling occurs. This is avoided by slits between flaps and the wing. As slats and flaps act similar to small wings, they inject air from below

Figure 9: Winglet of Condor with alula [3]

the wing to the top boundary layer, thus giving it more kinetic energy. This effect is even higher at reactive motor aeroplanes, as they make use of the gases, which come out of motor with high kinetic energy. Flaps are used to inject this gases into the top boundary layer. The amount of increasing the lift coefficient depends on the type (figure 10) and number of flaps and slats (figure 8,a). Increases tend to go even higher then 100% of lift

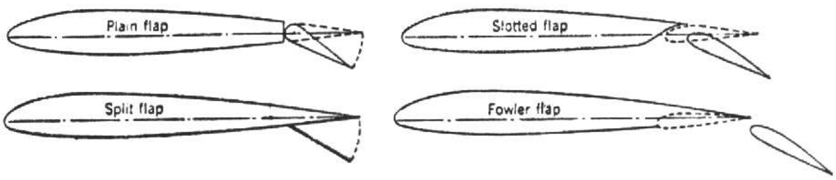

Figure 10: Different types of flaps (plain, split, slotted, fowler)[2]

by standard profile.
Although we are not observing the drag coefficient, we should remark, that flaps and slats induce a lot of drag. They are therefore used at take-offs and landings, but never at high velocities during the flight. Therefore, the wing must be able to change shape during the flight.

4.3 Micro vortex generators

Apart from flaps, other mechanisms can be found in nature, which prevent flow separation and make it possible to fly at low speeds. If one looks closely at the leading end of the owl's wing, one may observe leading edge comb. This is a set of wing extensions, forming a structure resembling a comb (figure 11).

Laminar flow separation can be prevented by making the flow turbulent through the use of turbulence generators or small protuberances at the leading edge such as feathers with filaments, comb teeth, or hairs standing perpendicular to the wing surface. By

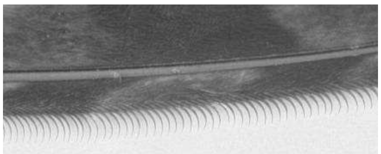

Figure 11: Owl's primary feathers leading edge comb [5]

observing an owl wing in a low speed tunnel, we can find out that at high angle of attack, the comb generates a stationary spanwise vortex sheet which extends from alula to the tip of the first primary feather, and prevents flow separation on the outer part of the wing.

If we introduce a comb like structure to the wing of an airplane, not only will it delay

Figure 12: Micro vortex generator technology [5]

stalling to lower magnitude of velocity, but also does not increase the drag coefficient[5]. It will also make flying silent[6]. This system of vortex generators is therefore highly usable in all stages of flight.

5 Conclusion

It has been shown, that lift coefficient can be increased by varying certain properties of the wing itself , or by installing new components (micro vortex generators). Obtaining

[5]The drag increases because of the produced vortices, but the initial drag is decreased because of decreased thickness of boundary layer.

[6]The noise, produced by the separation of the streamlines is decreased to low magnitude

higher values of the lift coefficient with optimal values of thereby induced drag is therefore not over yet. The solid vortex generators are being replaced by thin jets of air injected into the boundary layer perpendicular to its movement. In their case, we can regulate the amount of vorticity induced on the wing. And of course, we must still look for the mechanisms, made by nature, that are still hidden from our eyes.

6 References

1. Richard von Mises: Theory of flight, Dover Publications, New York, 1959

2. G. A. Tokaty: A History and Philosophy of Fluid Mechanics, Dover Publications, New York, 1994

3. A. Azuma: The Biokinetics of Flying and Swimming, Springer – Verlag Tokyo, 1992

4. Rudolf Podgornik: Mehanika kontinuov, Lecture notes, Ljubljana, 1999

5. Micro Aerodynamics inc., www.microaero.com

7 Appendix

A Relation vorticity – circularity

Let us examine the circulation of a simple circulating motion with solid rotating core (figure 13) [1, p.189] (to avoid infinite velocity in the centre of this motion). Outside the

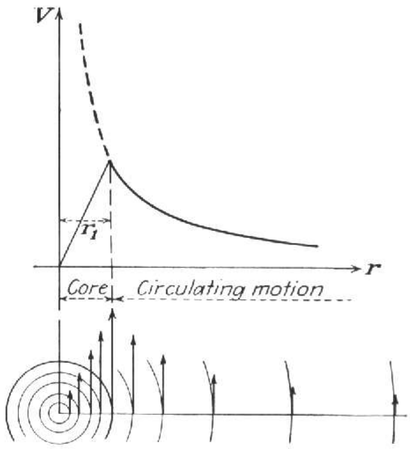

Figure 13: Circulating motion with solid rotating core [1]

circle with radius $r = r_1$ this modified stream pattern coincides with that of a circulating motion, the velocity distribution given by

$$V = \frac{\Gamma}{2\pi r} \qquad r \geqq r_1$$

Inside this circle $r = r_1$, the fluid rotates as a rigid body with the angular velocity

$$\omega = \frac{V_1}{r_1} = \frac{\Gamma}{2\pi r_1}^{2} \qquad r \leqq r_1 \tag{10}$$

Here the velocity is distributed according to

$$V = \omega r = \frac{\Gamma}{2\pi r_1^2} r \qquad r \leqq r_1$$

This condition assures the continuity of the velocity across the circle $r = r_1$.
Seen in space, the rotating core forms a thin circular cylinder, which is called the vortex filament. The double product of its angular velocity and area of its cross section is called its vorticity. According to equation (10) the vorticity in this case equals the circulation of the circulating motion prevailing outside the vortex filament. Thus a circulating motion may be conceived as attached to a straight vortex filament of the vorticity Γ.

If r_1 is made to tend toward zero, this vortex filament reduces to a straight vortex line of vorticity Γ. Thus we can create a uniform vortex sheet as a continuous distribution of vortex lines, each of infinitesimal vorticity, over a closed cylindrical surface. Doing that, one may arrive at an induced velocity distribution that is free of singularities [1, p.191].